Tyrosine Phosphorylation and Acetylcholine Receptor Cluster Formation in Cultured *Xenopus* Muscle Cells

Lauren P. Baker and H. Benjamin Peng

Department of Cell Biology and Anatomy, and the Curriculum in Neurobiology, University of North Carolina, Chapel Hill, North Carolina 27599

Abstract. Aggregation of the nicotinic acetylcholine receptor (AChR) at sites of nerve–muscle contact is one of the earliest events to occur during the development of the neuromuscular junction. The stimulus presented to the muscle by nerve and the mechanisms underlying postsynaptic differentiation are not known. The purpose of this study was to examine the distribution of phosphotyrosine (PY)-containing proteins in cultured *Xenopus* muscle cells in response to AChR clustering stimuli. Results demonstrated a distinct accumulation of PY at AChR clusters induced by several stimuli, including nerve, the culture substratum, and polystyrene microbeads. AChR microclusters formed by external cross-linking did not show PY colocalization, implying that the accumulation of PY in response to clustering stimuli was not due to the aggregation of basally phosphorylated AChRs. A semi-quantitative determination of the time course for development of PY labeling at bead contacts revealed early PY accumulation within 15 min of contact before significant AChR aggregation. At later stages (within 15 h), the AChR signal came to approximate the PY signal. We have reported the inhibition of bead-induced AChR clustering in response to beads by a tyrphostin tyrosine kinase inhibitor (RG50864) (Peng, H. B., L. P. Baker, and Q. Chen. 1991. *Neuron.* 6:237–246). RG50864 also inhibited PY accumulation at bead contacts, providing evidence for tyrosine kinase activation in response to the bead stimulus. These results suggest that tyrosine phosphorylation may play an important role in the generative stages of cluster formation, and may involve protein(s) other than or in addition to AChRs.

ONE of the earliest events to occur during the development of the neuromuscular junction (NMJ)[1] is the accumulation of nicotinic acetylcholine receptors (AChRs) within the postsynaptic membrane at sites of nerve–muscle contact (*3*). The accumulation of AChRs into dense aggregates containing 10,000 receptors/μm^2 or more (20) is crucial for the development of rapid and efficient signaling from nerve to muscle. The stimulus used by nerve to induce clustering, how it is transduced, and the molecular mechanism whereby receptors are clustered are not well understood. It is commonly believed that a factor secreted and/or presented to the muscle cell by nerve acts in a local manner to initiate clustering either directly, by effecting a change in AChRs or proteins associated with them (21), or indirectly, via the prior development of an adhesive cytoskeletal specialization (for review see reference 8). In addition to nerve, other stimuli used to study postsynaptic development include the culture substratum (2, 11), electric field (31, 37, 51), and brain- and muscle-derived factors including ARIA and agrin (19, 36, 55). In addition to effecting AChR clustering, most of these stimuli induce additional NMJ-like specializations, including the development of a synapse-specific basal lamina and the accumulation of intracellular receptor-associated and cytoskeletal proteins.

We have used polycation- and basic fibroblast growth factor (bFGF)-coated beads as spatially and temporally controllable stimuli for the induction of postsynaptic development in cultured *Xenopus* muscle cells (40, 42). bFGF-coated beads appear to present bFGF to specific receptors on the muscle cell surface, and AChR clustering induced by these beads is blocked by a member of the tyrphostin family of tyrosine kinase inhibitors (42), providing evidence for the involvement of tyrosine phosphorylation in these bead effects. Receptors for bFGF and other growth factors such as PDGF, EGF, and insulin are tyrosine kinases that are phosphorylated on tyrosine and activated upon ligand binding (for review see reference 57). Recently, we have demonstrated the potency of native, uncoated polystyrene beads in inducing postsynaptic development (6), and similar results have also been reported by Anderson et al. (4). Our data suggest that the effect of uncoated beads may be mediated by endogenous heparin-binding factors. The effect of these uncoated beads can also be blocked by tyrphostin (6). Thus, activation of an endog-

This work was previously presented in abstract form (Baker, L. P., and H. B. Peng. 1991. Soc. Neurosci. Abstr. 17:219).

1. *Abbreviations used in this paper*: AChR, Acetylcholine receptor; bFGF, basic fibroblast growth factor; NMJ, neuromuscular junction; PY, phosphotyrosine; R-BTX, rhodamine-conjugated α-bungarotoxin.

© The Rockefeller University Press, 0021-9525/93/01/185/11 $2.00

enous tyrosine kinase may be involved in AChR clustering induced by bFGF-coated and uncoated beads.

The nicotinic AChR is a pentamer consisting of four distinct subunits (14). The receptor possesses eight proposed or demonstrated phosphorylation sites (26, 47), and can be phosphorylated by several serine/threonine kinases, and by an endogenous tyrosine kinase in vitro and in vivo. Cyclic AMP-dependent protein kinase phosphorylates the δ and γ subunits (25), protein kinase C phosphorylates the α and δ subunits (28, 46), and an as yet unidentified protein tyrosine kinase(s) phosphorylates the β, γ, and δ subunits (28, 45). Phosphorylation of the receptor on serine and tyrosine residues increases the rate of receptor desensitization, and may thus play a role in the regulation of short-term receptor-channel properties (for review see reference 27). Tyrosine phosphorylation of the AChR has also been postulated to play a role in cluster formation and/or maintenance. Immunocytochemical demonstration of phosphotyrosine (PY) at AChR clusters in rat diaphragm and in *Torpedo* electric organ is innervation dependent, and is correlated with tyrosine phosphorylation of the β and δ subunits in rat, and the β, γ, and δ subunits in *Torpedo* as determined by Western blot analysis (45). In addition a recent study by Wallace et al. (56) shows that the application of agrin to cultured chick myotubes leads to a threefold increase in tyrosine phosphorylation of the β subunit, in addition to receptor aggregation.

In the present study, immunocytochemical methods were used to examine the distribution of PY in cultured *Xenopus* muscle cells in response to several clustering stimuli. The results suggest that AChRs, while not tyrosine phosphorylated when diffusely distributed, are colocalized with PY when clustered, regardless of the stimulus, including uncoated beads. Inhibition of PY accumulation at bead contacts by a tyrosine kinase inhibitor provides evidence for tyrosine kinase activation in response to the bead stimulus. In addition, a semi-quantitative determination of the time course for development of PY labeling relative to the formation of bead-induced AChR clusters revealed early PY accumulation before significant AChR aggregation, within the first minutes of bead–muscle contact. This suggests that tyrosine phosphorylation of other, nonreceptor proteins at or gathered into the contact site precedes and may be necessary for accumulation of AChRs.

Materials and Methods

Materials

Polystyrene microbeads were obtained from Polysciences Inc. (Warrington, PA). Rhodamine-, and biotin-conjugated α-bungarotoxin, and rhodamine- and FITC-conjugated avidin were from Molecular Probes, Inc. (Eugene, OR). The 4G10 monoclonal anti-PY antibody was purchased from Upstate Biotechnology, Inc. (Lake Placid, NY). The PY20 monoclonal anti-PY antibody was purchased from ICN Biomedicals, Inc. (Costa Mesa, CA). Rhodamine- and FITC-conjugated goat anti-mouse secondary antibodies were from Organon Technika Corporation (Durham, NC). *O*-phospho-L-tyrosine was purchased from Sigma Chemical Co. (St. Louis, MO). RG50864 (active tyrphostin) and RG50862 (inactive tyrphostin) were provided by Rorer Central Research (King of Prussia, PA). Materials not listed here are noted in the text.

Preparation of Muscle Cultures

Muscle cell cultures were prepared according to a published protocol (43). Briefly, *Xenopus* embryos from stages 22–24 were freed from surrounding jelly coats and vitelline membranes, and the dorsal, myotomal portions were dissected away. The skin was removed by a 30-min incubation in calcium- and magnesium-free Steinberg solution (60 mM NaCl, 0.7 mM KCl, 0.4 mM EDTA, 10 mM Hepes, pH 7.4). The myotomal tissue was then dissociated with a second 30-min incubation in calcium- and magnesium-free Steinberg solution. After gentle trituration and removal of the undissociated dorsal portions, cells were plated onto glass coverslips and grown in Steinberg medium (60 mM NaCl, 0.7 mM KCl, 0.4 mM $Ca(NO_3)_2$, 0.8 mM $MgSO_4$, 10 mM Hepes, pH 7.4, supplemented with 10% L-15 medium, 1% FBS, and 0.1 mg/ml gentamycin). Cultures were kept at 22°C for 1 d to facilitate plating, and then maintained at 15°C. Cultures were generally used within 2–7 d of plating.

Preparation of Uncoated Beads and Induction of AChR Clusters

10-μm polystyrene microbeads were washed for 30 min in 95% ethanol, rinsed three times in distilled water, and brought up in 0.1 M PBS. Beads were either applied immediately to muscle cultures, or stored at 4°C for up to a week.

Beads were applied to muscle cultures via micropipette. Cultures were immersed in just enough culture medium to cover them. After application, beads were allowed to settle onto the cells for 30–60 s. Cultures were then rinsed in culture medium and incubated for 15 min–48 h at 23°C. Previous experiments have demonstrated that uncoated beads are still effective when applied to cells bathed in serum-free medium, thus ruling out the possibility that serum components adsorb to the beads and nonspecifically induce AChR clustering (6).

AChR clusters were visualized by labeling cultures before or after bead incubation. For prebead labeling, cultures were incubated in 300 nM rhodamine-conjugated α-bungarotoxin (R-BTX) in culture medium for 30 min, followed by two 5-min washes in culture medium. For postbead labeling, cultures were fixed according to the immunolabeling protocol (below), followed by two 10-min washes in PBS, and then incubated for 30 min in 300 nM fluorescent BTX, followed by two 5-min washes in PBS and PY immunolabeling.

External Cross-linking of AChRs

AChR microclusters were induced to form according to a protocol by Axelrod (5). Cultures were incubated in 4 μg/ml biotinylated α-bungarotoxin in culture medium for 15 min, rinsed twice in culture medium, and incubated in 4 μg/ml FITC- or rhodamine-avidin. After two rinses, cultures were incubated at 23°C for 6–8 h. The longer incubation period necessary to induce microclusters in these cells, beyond the 30–60-min incubation reported for rat myotubes (5) is likely due to species and culture differences; our experiments on *Xenopus* cells were performed at 23°C, as opposed to 37°C used for mammalian culture. Cells were then fixed according to the immunolabeling protocol (below) and processed for PY immunolabeling. As a control for specificity of the biotinylated BTX and the fluorescent avidin, cultures were incubated in 10 μg/ml unlabeled BTX, followed by biotinylated BTX and fluorescent avidin.

Immunocytochemistry

To visualize PY, cultures were fixed in −20°C, 95% ethanol for 3 min, followed by two 10-min washes in PBS. In some cases cultures were fixed in Luther's fixative (30) (0.5% paraformaldehyde, 80 mM cyclohexylamine in 10 mM Pipes buffer containing 10 mM $MgCl_2$ and 10 mM EGTA, pH 6.5) for 40 min, washed and permeabilized for 1 h in washing buffer (10 mM $MgCl_2$ and 10 mM NaN_3 in 75 mM Tris-HCl, pH 6.7) plus 0.5% Brij 58 (Sigma Chemical Co.). Nonspecific binding sites were blocked by a 15–60-min incubation in blocking buffer (10 mM $MgCl_2$, 10 mM NaN_3, and 0.1% BSA in 20 mM Tris-HCl, pH 6.5). Cells were labeled with either the 4G10 (13 nM) or PY20 (130 nM) monoclonal anti-PY antibodies in blocking buffer for 30 min, washed for a total of 20 min in blocking buffer, incubated in 133 nM FITC- or rhodamine–goat anti–mouse secondary antibody for 30 min, washed in PBS, and mounted in FITC-Guard (Testog, Chicago, IL) or 5% *n*-propyl gallate (Sigma Chemical Co.) in glycerol to minimize bleaching of the fluorescence signals. The sensitivity of the PY20 antibody proved to be significantly less than that exhibited by the 4G10 antibody. Therefore, the 4G10 antibody was used for all experiments except where noted in figure legends. As a control for specificity, the anti-PY antibody was preabsorbed with 10 mM *O*-phospho-L-tyrosine before application to selected cultures. This completely abolished all labeling.

Image Analysis of Fluorescence Labeling

Fluorescence images were obtained using a SIT camera attached to a Leitz Orthoplan microscope and a high resolution monitor, digitized, and subsequently analyzed using an Image-1 imaging system (Universal Imaging Corporation, West Chester, PA). After background subtraction, FITC-PY and R-BTX images from the same cell were paired side by side. Values were obtained for average gray scale intensity and area (pixels) for delineated bead-associated FITC-PY and R-BTX regions. Intensity values for background staining at sites adjacent to but not associated with bead-muscle contacts were also obtained, and used to subtract out baseline cell labeling at FITC and rhodamine wavelengths. Intensity values obtained from 55 cells per time point over several experiments were normalized and averaged with respect to the 48-h time point for analysis of intensity change over time. For comparison of rhodamine with FITC intensities, R-BTX values were multiplied by a correction factor to control for potential bias in the imaging system due to differential camera sensitivity, differential quantum yield of the rhodamine and FITC fluorophores, and for differential fluorophore-protein ratios for R-BTX and FITC-goat anti-mouse IgG. This correction factor was derived by determining the intensity of equimolar volumes of either R-BTX or FITC-goat anti-mouse IgG at concentrations that displayed a linear concentration/intensity relationship. 10 μl of either fluorophore in PBS was applied to a slide and coverslipped. A linear concentration/intensity relationship was observed from 50 to 300 nM, with a R-BTX/FITC-IgG ratio of 0.75. R-BTX values were then multiplied by 1.33.

The relative size of the R-BTX- and FITC-PY-labeled zones at developing bead-muscle contacts was determined by measuring the area (in pixels) of the R-BTX and FITC-PY fluorescence using the imaging system. Values were averaged and normalized to the 48-h R-BTX value, at which point the R-BTX and FITC-PY signals were extensively colocalized. Pixel values were then converted to μm^2.

Quantification of the percentage of bead-muscle contacts exhibiting R-BTX or FITC-PY labeling was carried out separately by conventional fluorescence microscopy without the use of computerized image analysis. The number of bead-muscle contacts per cell was quantified, and each contact was scored with respect to presence or absence of R-BTX and FITC-PY labeling.

Inhibition of PY Accumulation by Tyrphostin

RG50864 (active) or RG50862 (inactive) tyrphostin solutions were prepared from a 40-mM stock in DMSO, stored at −80°C. Working solutions (80 μM) were prepared in culture medium. Cultures were pretreated with culture medium (SM/DMSO), RG50862, or RG50864 for 3 h, and were maintained in these respective solutions during the subsequent uncoated bead incubation period. Sister cultures pretreated with RG50864 for 3 h were returned to culture medium for the ensuing bead incubation period, to study the reversibility of the drug treatment. Incubation of the beads themselves in RG50864 had no effect on the ability of these beads to induce clustering (6). After 16-h bead incubation, cultures were fixed and processed for FITC-PY immunolabeling and quantified with respect to the percentage of bead contacts demonstrating detectable PY labeling. Control cultures (SM/DMSO) were treated with 0.2% DMSO is culture medium (the concentration used in the tyrphostin working solutions).

Results

Immunolocalization of PY at AChR Clusters

Muscle cell cultures were prepared from stage 22–24 *Xenopus* embryos, and AChR clusters were induced to form in response to several stimuli, including nerve, the culture substratum, and uncoated polystyrene microbeads. AChRs were labeled with R-BTX, and PY-containing proteins were visualized using two mouse monoclonal anti-PY antibodies (mAbs 4G10 and PY20), followed by an FITC-conjugated secondary antibody. Cholinergic neurons present in these culture preparations formed contacts with muscle cells within several days, as described previously (3), resulting in the accumulation of AChRs at or near the sites of neurite contact. These contacts exhibited PY labeling along the extent of the receptor aggregates, as shown in Fig. 1, *A* and *E*.

Cultured aneural muscle cells form large, diffuse accumulations of AChRs, termed hot spots, on their ventral surface at sites of close membrane–substratum apposition. Similar to clusters induced by nerve and beads, hot spots are composed of smaller aggregates of AChRs, and often display an intricate labeling pattern (39, 40). Like the labeling observed at nerve–muscle contacts, PY was dramatically colocalized with AChRs at these specializations (Fig. 1, *B* and *F*). Colocalization was also observed at smaller, dorsal hot spots which are also observed in culture (data not shown). Labeling for AChRs and PY was generally co-extensive, conforming to the substructural pattern of AChR clusters discernible at the light microscopic level. However, hot spots were also observed in which the labeling patterns did not overlap as tightly. In these instances, the PY labeling displayed a more restricted pattern than the AChRs, such that some receptor-rich regions were not associated with PY (Fig. 2).

To study bead-induced specializations, cultures were seeded with uncoated polystyrene beads and incubated for 24 h. Here too, extensive colocalization of PY with AChR clusters was observed (Fig. 1, *C* and *G*). In addition to uncoated beads, beads coated with polyornithine and bFGF also induced AChR clusters with coincident PY accumulation (data not shown). Control cultures in which the anti-PY antibody was preabsorbed with 10 mM *O*-phospho-L-tyrosine did not exhibit any labeling (Fig. 1, *D* and *H*). Also, cells fixed with paraformaldehyde but not permeabilized did not show any immunolabeling, demonstrating that the PY accumulation was intracellular.

Distinct PY immunolabeling was not limited to receptor clusters. Along the extent of the sarcolemma, a light, punctate labeling pattern was observed at the cell surface (Figs. 1 *F* and 2 *C*). In addition, increased PY labeling was sometimes observed at sites of cell–cell contact (see Fig. 4 *C*), as previously reported by Maher et al. (32). Preabsorption of the primary antibody with excess *O*-phospho-L-tyrosine also eliminated all of these types of labeling.

Significantly, fibroblast-like cells also responded to the application of uncoated beads by the formation of bead-associated PY labeling (Fig. 3, *B* and *C*). This labeling developed with a similar time course to that seen at bead–muscle contacts (discussed below). In keeping with the fact that these cells lack AChRs, no corresponding R-BTX labeling was observed at these sites. Fibroblast-like cells also displayed significant PY immunolabeling at sites of focal adhesion (Fig. 3 *A*), as previously reported (32). In fibroblasts, these structures are enriched in actin and actin-associated proteins, several of which can be phosphorylated on tyrosine (18, 22, 24, 29, 38, 49).

Cross-linked AChRs Are Not Associated With PY

To determine whether prephosphorylated AChRs are responsible for the accumulation of PY at AChR clusters, cultured muscle cells were induced to form AChR microclusters according to a protocol by Axelrod (5). Incubation of cultures in biotinylated BTX, followed by FITC–avidin and a 6–8-h incubation period resulted in the formation of visible microclusters ~1 μm in diameter (Fig. 4 *B*). Preincubation in 10 μg/ml unlabeled BTX, followed by biotinylated BTX and FITC-avidin completely abolished the formation of these microclusters (Fig. 4 *D*). Immunolabeling of these cultures

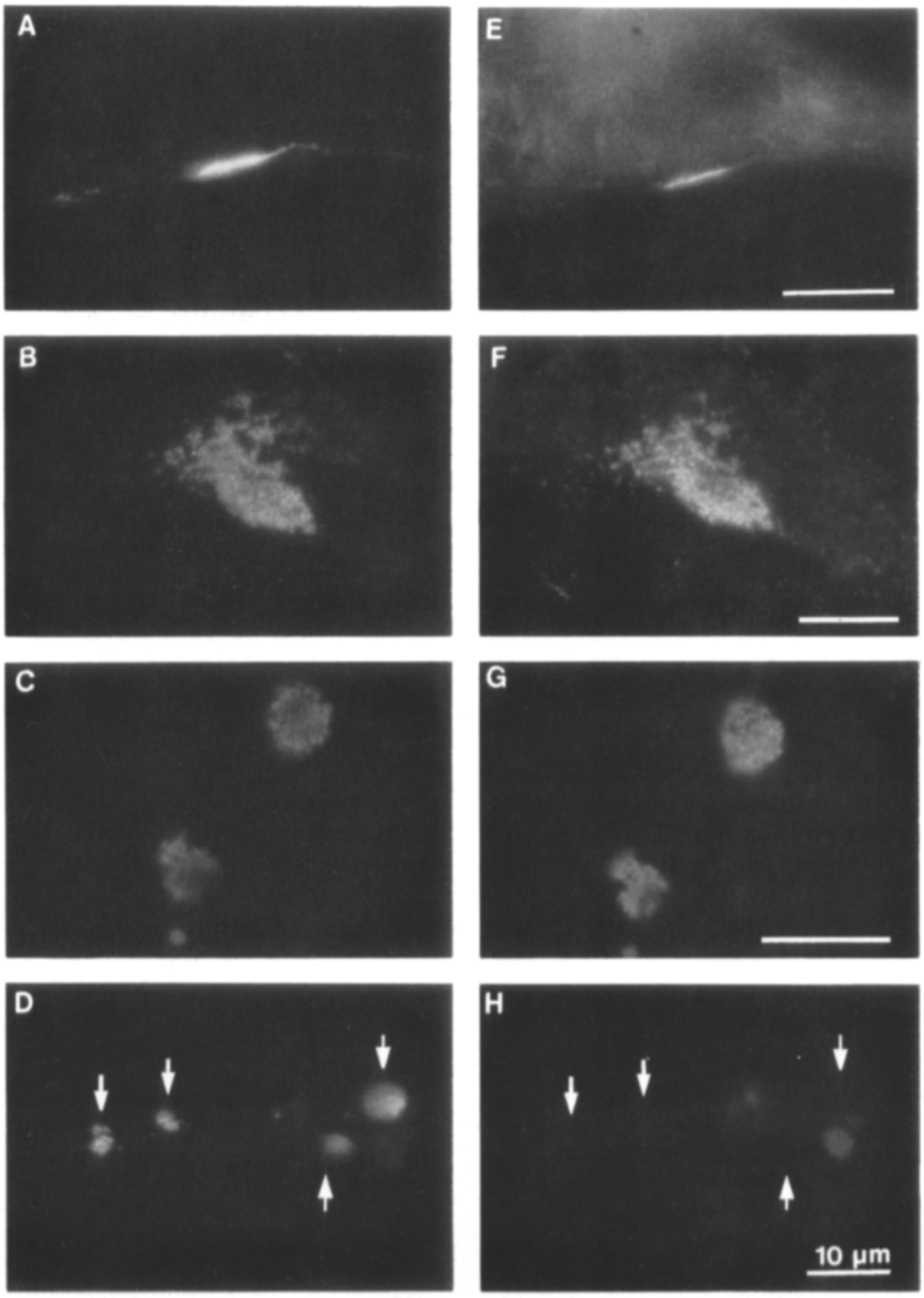

Figure 1. Immunocytochemical demonstration of PY at AChR clusters induced by nerve, culture substratum, and uncoated polystyrene beads. AChRs were visualized with R-BTX (*A–D*). PY was visualized with anti-PY mAb PY20 (*E*), and 4G10 (*F–H*), followed by an FITC-conjugated goat anti-mouse secondary antibody. (*A* and *E*) Neuromuscular junction formed in culture; (*B* and *F*) AChR cluster (hot spot) formed on the ventral surface of a muscle cell; (*C* and *G*) uncoated bead-induced clusters; (*D* and *H*) bead-treated culture immunolabeled with anti-PY antibody preabsorbed with 10 mM *O*-phospho-L-tyrosine. Arrows show bead-induced AChR accumulation (*D*), and lack of PY at bead contacts in preabsorbed control (*H*). Left column, R-BTX. Right column, FITC–PY. Bar, 10 μm.

with the anti-PY antibody followed by a rhodamine-conjugated secondary antibody resulted in labeling of hot spots and regions of cell–cell contact (Fig. 4, *B* and *C*). However, the induced AChR microclusters did not label for PY (Fig. 4 *C*). Similar results were obtained when the rhodamine and FITC fluorophores were switched (R-avidin and FITC-PY). This suggests that diffusely distributed AChRs are not phosphorylated on tyrosine, and that the accumulation of PY at AChR clusters is not due to the aggregation of basally phosphorylated AChRs.

Development of PY Accumulation at AChR Clusters

Experiments were carried out to determine the time course for the development of PY accumulation relative to the development of AChR clusters in muscle cells, using uncoated beads as the stimulus. Beads were applied to cultures for periods ranging from 15 min to 48 h, and cultures were labeled with R-BTX before or after bead incubation, with similar results. Prelabeling before bead application was performed to ensure that failure to detect AChRs was not due to hindered access of R-BTX to AChRs. The cells were then fixed and processed for PY immunocytochemistry.

The number of bead–muscle contacts per cell was counted, and each contact was scored with respect to the presence or absence of R-BTX and PY labeling (Fig. 5). By 15 min of bead incubation, ~15% of contacts exhibited PY accumulation (Fig. 5). This early PY labeling was somewhat diffuse,

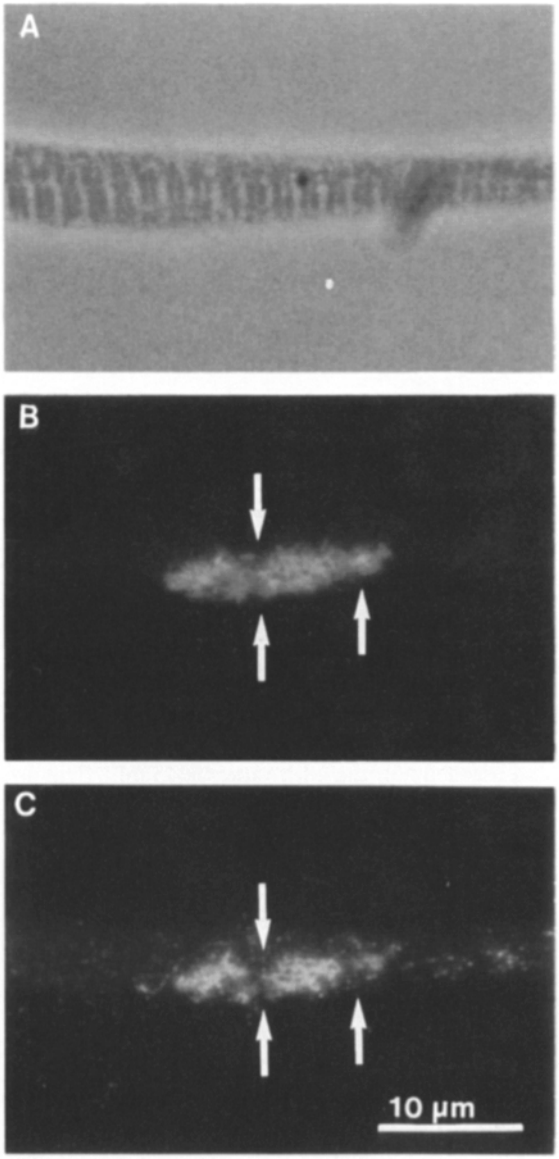

Figure 2. Differential labeling pattern observed at a ventral hot spot. (*A*) Phase-contrast; (*B*) R-BTX; and (*C*) FITC-PY (4G10). Note the more restricted PY labeling as compared with R-BTX labeling. Arrows point to regions of AChR accumulation (*B*) in the absence of PY labeling (*C*). Bar, 10 μm.

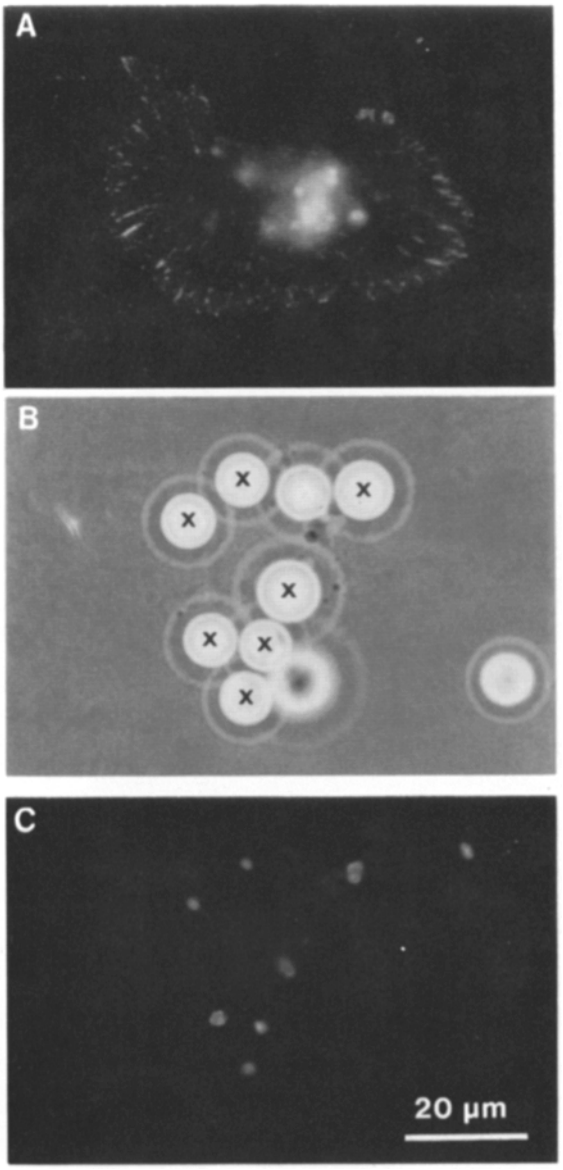

Figure 3. PY immunolabeling of fibroblast-like cells. (*A*) FITC-PY (PY20). Note the distinct labeling at sites of focal adhesion. The bright structures in the center of the cell are autofluorescent yolk granules. (*B*) Different cell from the same culture, contacted by several uncoated beads, phase-contrast. (*C*) FITC-PY (4G10) image of *B* showing accumulation of PY at sites of bead contact within 15 min. Bead contacts at the cell surface are at a different focal plane from focal adhesions located at the ventral cell surface. Thus, focal adhesions are not visible in this image. The fluorescence at the far right of *C* is a noncellular fluorescent particle not associated with a bead contact. Beads marked with black x's (*B*) induced FITC-PY accumulation (*C*). Bar, 20 μm.

but conformed to the size and shape of the beads, and was particularly striking at sites where beads made contact with dorsal regions of broad flattened cells (bFGF-coated beads also induced this early accumulation of PY, data not shown). The percentage of beads demonstrating PY accumulation increased steadily to plateau at ~70% within 15 h, with a half-maximal percentage attained at ~45 min. R-BTX labeling, on the other hand, could be detected at <5% of contacts by 30 min. This percentage increased to plateau within 15 h, with a half-maximal percentage attained at ~3 h, at which time all contacts which showed PY labeling also showed R-BTX labeling. Similar results were obtained when the rhodamine and FITC fluorophores were switched (FITC–BTX and R-PY), demonstrating that the early detection of PY at bead contacts was not due to greater visibility/detectability of the FITC fluorophore over the rhodamine fluorophore.

To further characterize this early phosphorylation event, a semi-quantitative assay of the relative intensities of R-BTX–labeled AChRs and FITC-PY at different time points was carried out. Fluorescence images were obtained and analyzed using a digital imaging system. The intensity data averaged from 55 cells per time point was normalized to the data obtained at the 48-h time point for both the rhodamine and the FITC signals (Fig. 6 *A*). The averaged FITC–PY signal reached ~45% of its 48-h value by 15 min of bead–muscle

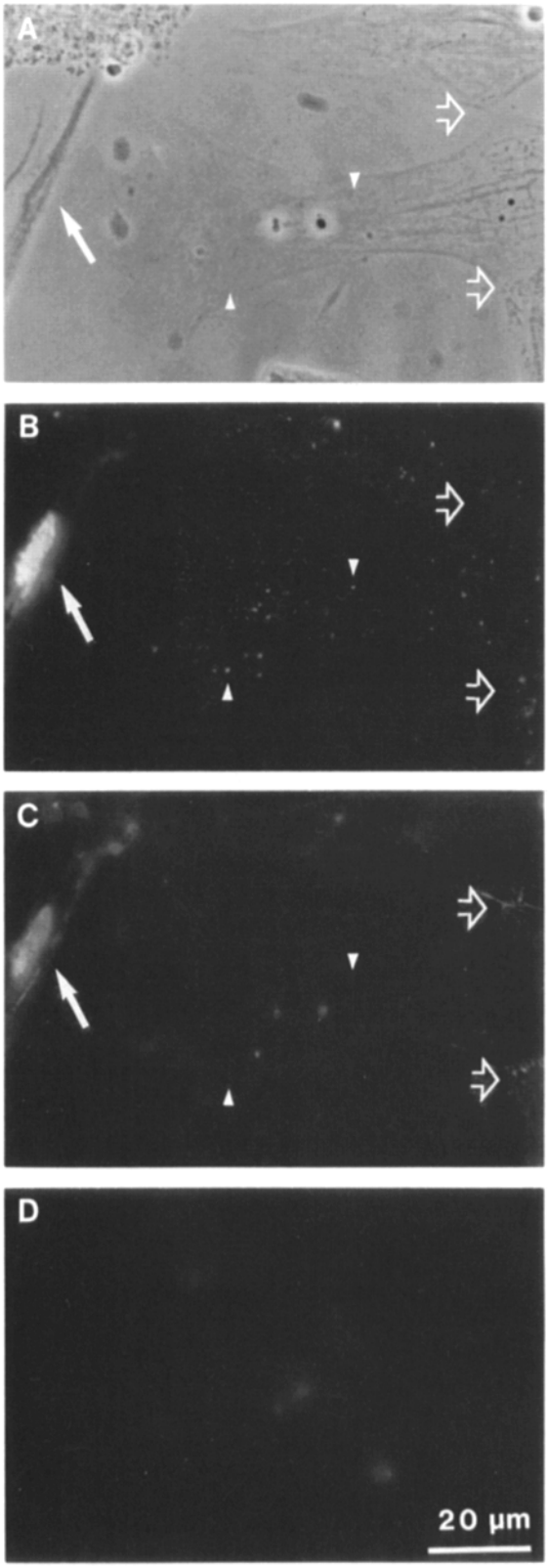

Figure 4. AChR microclusters do not demonstrate PY labeling. Cells were labeled with biotinylated BTX followed by FITC–avidin, and incubated for 6 h before fixation and processing for immunocytochemistry. (*A*) Phase-contrast. Three muscle cells are visible, in addition to a portion of a melanocyte. (*B*) AChR microclusters visualized with FITC–avidin. (*C*) Rhodamine-PY (4G10) immunolabeling, showing no PY colocalization with AChR microclusters. (*D*) Control culture preincubated with 10 μg/ml unlabeled BTX before being subjected to the cross-linking protocol. Open arrowheads indicate sites of cell–cell contact between two muscle cells (*B* and *C*). Solid arrowheads indicate representative AChR microclusters (*B*). Solid arrows point to an AChR hot spot formed on the ventral surface of one of the muscle cells. Bar, 20 μm.

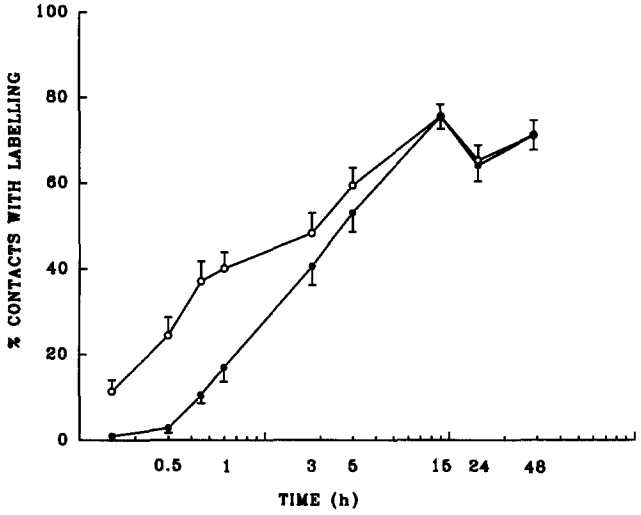

Figure 5. Percentage of bead–muscle contacts displaying R-BTX or FITC-PY (4G10) labeling over time. Time points are 15, 30, 45, 60 min, 3, 5, 15, 24, and 48 h. Each point represents the mean ± SEM of 40 cells over two time course experiments. A total of 360 cells were counted. FITC-PTYR (○); RBTX (●).

contact, and reached half the 48-h value by 45 min. The increase in FITC intensity over the time course ranged 55 gray value units. By comparison, the averaged R-BTX signal reached only 10% of its 48-h value by 15 min, and reached half the 48-h value after 5 h. The increase in rhodamine intensity over the time course ranged 90 gray value units. Whereas the percentage of bead contacts displaying either signal reached a maximum by 15 h, corresponding intensities never plateaued during the extent of the time course, suggesting a maturation process which continues beyond 48 h.

To compare the intensity of the two fluorescence signals, the data were corrected for bias in the imaging system as described in Materials and Methods. This controlled for differential SIT camera sensitivity at the rhodamine versus the FITC wavelengths, differential quantum yield of the rhodamine versus FITC fluorophores, and differential fluorophore–protein ratio for the rhodamine-tagged bungarotoxin (BTX) versus the FITC-tagged secondary antibody. The ratio of the fluorescence signals was then calculated (Fig. 6 *B*). The R-BTX intensity was ~20–25% of the FITC-PY intensity during the first 60 min of bead–muscle contact. Thereafter, the R-BTX intensity increased to reach 100% of the FITC value within 5 and 15 h. It then surpassed the FITC intensity and appeared to reach a plateau at 150% of the FITC value by 24 h. By comparison, spontaneously formed hot spots showed a similar ratio (120%) to these relatively well-formed bead-induced clusters (Fig. 6 *B*).

In an attempt to enhance the AChR signal at early bead

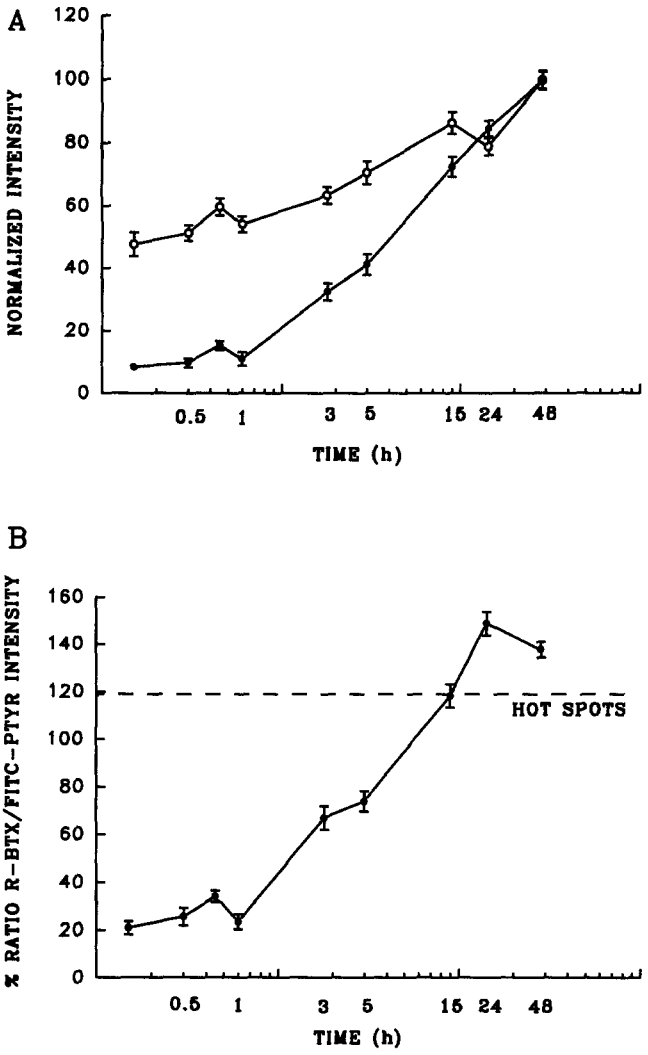

Figure 6. Development of R-BTX or FITC-PY (4G10) intensity at bead–muscle contacts over time. (*A*) Normalized values for R-BTX and FITC-PY were plotted individually. FITC-PTYR (○); R-BTX (●). (*B*) Values in *A* corrected for system bias and replotted as a percent ratio of R-BTX to FITC-PY. Time points are 15, 30, 45, 60 min, 3, 5, 15, 24, and 48 h. Each point represents the mean ± SEM of 55 bead–muscle contacts over three time course experiments. In *B*, the dotted line represents the average intensity ratio for spontaneous AChR hot spots. A total of 495 bead–muscle contacts were analyzed.

contacts (15 min–1 h), AChR labeling was amplified using a mAb generated against the cytoplasmic portion of the AChR (88b; from Dr. Stanley Froehner, UNC Chapel Hill), followed by an FITC secondary antibody. This procedure failed to reveal any early AChR signal which was not previously detected by the R-BTX labeling, and the time course for AChR accumulation using this labeling procedure was similar to that obtained with R-BTX.

With respect to the size of developing bead-induced clusters, the earliest detectable FITC-PY accumulation averaged ~4.5 μm^2 between 15 min and 3 h, and increased in size to average ~5.2 μm^2 from 5–48 h (Table I). R-BTX labeling, when present, averaged ~75% of the FITC-PY area over the first 5 h. By 15 h, R-BTX labeling became 100% congruent with FITC-PY labeling. A composite showing representative examples of R-BTX and FITC-PY digitized images at various time points is presented in Fig. 7.

Table I. Relative Size of PY Versus AChR Labeling at Bead Contacts

Time	FITC area (μm^2)	RH area (μm^2)	% RH/FITC
15 min	4.55	3.90	87.58
30 min	4.41	3.09	70.97
45 min	4.24	3.39	82.10
1 h	4.67	2.51	57.33
3 h	4.61	3.22	70.68
5 h	5.33	3.96	76.29
15 h	5.08	4.81	98.27
24 h	4.61	5.16	112.26
48 h	5.95	5.95	101.19
Hot spots	14.35	17.38	126.15

Average values are presented for each time point. The percent ratios of R-BTX/FITC-PY (% RH/FITC) were calculated individually for each bead contact examined, and vary minimally from the ratio of averaged values presented for columns 3 (RH area) to 2 (FITC area). Note the increase in % RH/FITC from ~75% to ~100% after 15-h bead–muscle contact. An average of 45 bead contacts were examined per time point over three experiments. A total of 404 contacts were examined. Similar values for AChR hot spots are included (n = 55).

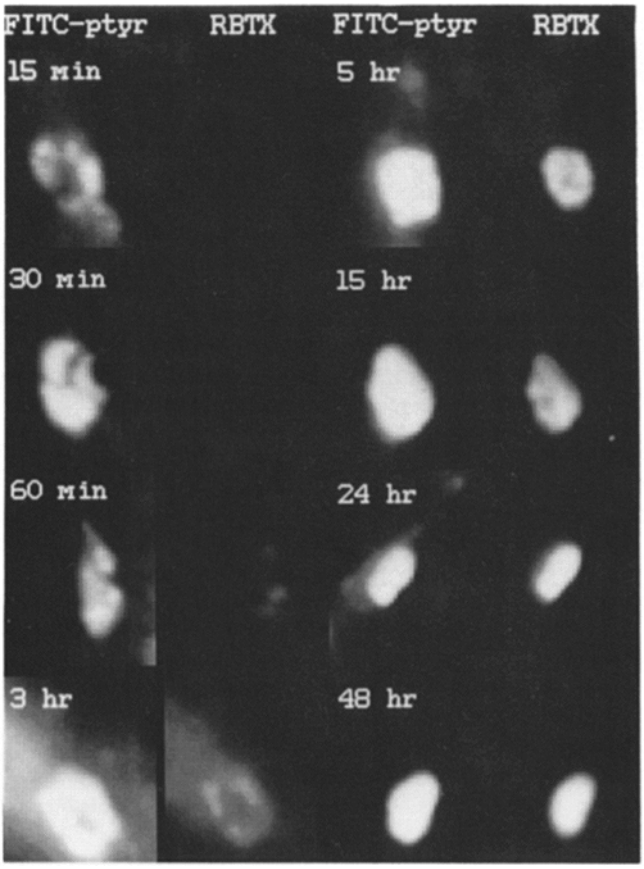

Figure 7. Comparison of R-BTX versus FITC-PY (4G10) over time using digitized fluorescence images. R-BTX and FITC-PY images of bead–muscle contacts and the time after bead application are indicated.

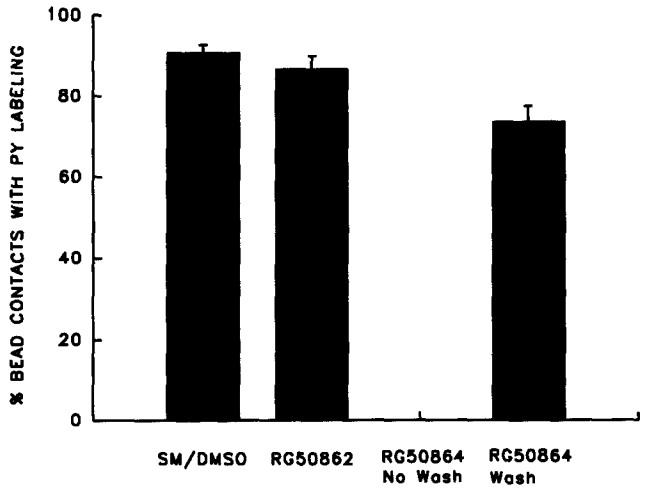

Figure 8. Inhibition of PY accumulation at uncoated bead-muscle contacts by tyrphostin (RG50864). Cultures were pretreated with culture medium (SM/DMSO), RG50864 (active), or RG50862 (inactive) for 3 h, and maintained in these respective solutions during a subsequent 16-h incubation with uncoated beads. Control cultures (SM/DMSO) demonstrated 91% of uncoated bead contacts with PY immunolabeling. Cultures treated with an inactive tyrphostin (80 μM RG50862) showed PY labeling at 87% of bead contacts. Cultures treated with 80 μM RG50864 showed complete inhibition of PY accumulation at bead contacts. A 16-h wash in culture medium after a 3-h pretreatment with RG50864 led to a recovery of PY accumulation in sister cultures to ~74% of contacts. Values show mean percentage ± SEM of bead contacts with PY labeling. n = 60 cells for each treatment group.

Inhibition of PY Accumulation at Bead Contacts by Tyrphostin

We have previously demonstrated inhibition of bFGF-coated and uncoated bead-induced AChR clustering by a member of the tyrphostin family of tyrosine kinase inhibitors (RG50864) (6, 42). The effect of this compound on the PY accumulation at bead–muscle contacts was therefore ascertained. Cultures were preincubated in 80 μM RG50864 for 3 h and maintained in this solution during the subsequent 16-h bead incubation period. This treatment led to a complete inhibition of bead-induced PY accumulation relative to untreated cultures or cultures treated with an inactive tyrphostin (RG50862; Fig. 8). Treatment of uncoated beads themselves with RG50864 has no effect on their ability to induce AChR clustering (6). A 16-h wash in culture medium following 3-h RG50864 preincubation resulted in recovery of sister cultures to 81% of the untreated (SM/DMSO) value, showing that the inhibition by RG50864 was not due to cytotoxic effects. We have also determined that a 3-h preincubation in RG50864 is sufficient to reversibly inhibit PY accumulation during a subsequent 1-h bead incubation (data not shown). Thus, RG50864 was able to inhibit the PY accumulation at early as well as relatively mature uncoated bead contacts, providing evidence for an increase in tyrosine kinase activity in response to the bead stimulus.

Discussion

Although many of the major events underlying the development of the NMJ, such as the accumulation of AChRs and acetylcholinesterase, have been well characterized, the mechanisms underlying this process are unknown. Previous studies have implicated a tyrosine phosphorylation mechanism in aspects of synapse formation and/or function (42, 45, 56). The purpose of this study was to examine the distribution of PY in *Xenopus* muscle cells in response to AChR clustering stimuli. Our results are as follows: (*a*) PY immunolabeling accumulated at AChR clusters induced by several stimuli, including nerve, the culture substratum, and polystyrene beads. In addition, PY was also observed in fibroblast-like cells at sites of bead contact. (*b*) AChR microclusters induced by cross-linking did not demonstrate colocalized PY. (*c*) A distinct accumulation of PY at early uncoated bead-muscle contacts was observed before significant AChR aggregation. (*d*) A tyrphostin tyrosine kinase inhibitor reversibly blocked PY accumulation at bead–muscle contacts.

In this study, we focused on polystyrene microbeads as a convenient stimulus which provides temporal and spatial control over the formation of AChR clusters and other postsynaptic specializations (40, 42). In addition to polycation- and bFGF-coated beads, uncoated beads that have not been treated with proteins are also effective in inducing postsynaptic differentiation (4, 6). Our data have suggested that these beads may act by presenting a preexisting cell-surface or extracellular matrix-bound factor(s) to specific receptors on the muscle cell surface (6).

The accumulation of PY at AChR clusters induced by various stimuli indicates that tyrosine phosphorylation is a common feature of AChR clusters. PY was observed at relatively mature clusters, induced by nerve and the culture substratum, as well as at bead contacts during the earliest stages of postsynaptic differentiation. The lack of colocalized PY labeling at AChR microclusters formed by cross-linking suggests that AChRs in the diffuse or nonclustered state are not significantly phosphorylated on tyrosine, within our limits of detection, and the observed PY accumulation at AChR clusters is not due to the aggregation of basally phosphorylated AChRs. This correlates well with previous biochemical studies in which cultured aneural myotubes and denervated muscle in vivo, both of which possess diffusely distributed receptors, were found to exhibit only a very low level of AChR-associated PY, whereas AChRs from innervated muscle were associated with a high level of PY (34, 45). Upon microscopic inspection microclusters appeared to be localized to the cell surface, and not to be aggregated into intracellular compartments. However, our experiments did not differentiate definitively between cell-surface and and internalized AChRs, and it is possible that basally phosphorylated AChRs were microclustered and internalized, only to be subsequently dephosphorylated. It is also possible that the process of cross-linking itself resulted in dephosphorylation of basally tyrosine phosphorylated AChRs. Future biochemical studies will be aimed at determining directly the phosphorylation level of AChRs in unstimulated cells and in cells induced to form microclusters.

The results of this study showing inhibition of PY accumulation at bead contacts by tyrphostin, taken together with our previous results demonstrating inhibition of bead-induced AChR clustering by this compound (6, 42), indicate a specific increase in tyrosine kinase activity in response to the bead stimulus. Two results from this study suggest that bead

contact induces phosphorylation of proteins other than the AChR: the accumulation of PY at early bead contacts before detectable accumulation of AChRs, and the larger size of PY-labeled zones relative to R-BTX labeled zones up to 15 h of bead contact. An early accumulation of PY has also been observed at sites of presumptive AChR clustering in response to stimulation with electric field (43a). At later stages of bead contact, when there is a more or less exact colocalization between R-BTX and PY labeling, the AChR is presumably a substrate for tyrosine phosphorylation.

The possibility exists that tyrosine-phosphorylated AChRs are in fact significantly accumulated at early bead contacts but remain undetectable by R-BTX labeling. If the observed PY immunolabeling does reflect phosphorylated AChRs alone, the intensity ratio obtained in this study would suggest that during early stages of bead-induced cluster formation AChRs are highly phosphorylated on tyrosine, and much less so at later stages (by 24 h). However, amplification of the AChR signal with an anti-AChR mAb followed by an FITC-secondary antibody failed to reveal any enhanced AChR signal at early bead–muscle contacts. In addition, available evidence suggests that the amount of PY associated with AChRs increases with time after stimulus application; agrin leads to a threefold increase in tyrosine phosphorylation of the β subunit within 3 h (56), and AChRs isolated from innervated, as opposed to denervated adult muscle, are tyrosine phosphorylated on the γ and δ subunits in addition to the β subunit (45).

The basis for the differential PY labeling pattern at spontaneously formed hot spots, where portions labeled with R-BTX were often not associated with PY (Fig. 2) is unknown. Given that the AChR is a substrate for tyrosine phosphorylation in other systems, the more restricted PY labeling suggests that there is a subset of AChRs which are not phosphorylated, even when clustered. Alternatively, the PY labeling at hot spots may correspond to non-AChR proteins.

Possible Non-AChR Substrates for Tyrosine Phosphorylation

The early accumulation of PY at sites of presumptive AChR aggregation suggests a role for non-AChR phosphoproteins in the initial stages of synaptogenesis. Possible non-AChR substrates for tyrosine phosphorylation include (*a*) cytoskeletal proteins, and (*b*) regulatory proteins: receptor and nonreceptor tyrosine kinases, and their corresponding substrate proteins/kinases.

The Cytoskeleton

Early electron microscopic studies of the NMJ showed a thickening of the postsynaptic sarcolemma along with the accumulation of 5–10-nm filamentous structures (16). Actin was later identified as a major postsynaptic protein at the NMJ (23). Since these initial demonstrations, other studies have shown a similar cytoskeletal specialization and actin accumulation at postsynaptic sites induced by various stimuli (9, 44). An early cytoskeletal meshwork has been detected at bead–muscle contacts as well, before AChR aggregation (41). Experimental disruption of actin filaments results in a loss of cluster stability and a reorganization of previously aggregated AChRs within the plasma membrane (9, 15, 52). As a result of these and other studies, it has been postulated that the deposition of an actin cytoskeletal meshwork may act to trap diffuse AChRs at sites of presumptive cluster formation, or to stabilize developing AChR aggregates via interaction with other proteins (8).

Several actin-associated cytoskeletal proteins that were initially characterized at fibroblast focal adhesions are also concentrated at postsynaptic sites. These proteins include vinculin, talin, paxillin, and integrin (7, 10, 48, 54), all of which are substrates for the *src* kinase in fibroblasts transformed by the Rous sarcoma virus (RSV; 18, 22, 24, 29, 38, 49). PY immunolabeling has been demonstrated at residual focal contacts in RSV-transformed fibroblasts (22), which demonstrate dramatic cytoskeletal alterations and changes in adhesion (for review see reference 12), as well as at focal contacts in normal fibroblasts (32). Paxillin, and another protein found at focal adhesions, tensin, are phosphorylated on tyrosine in untransformed cells in culture (17, 53). In addition, tyrosine phosphorylation of paxillin has been reported during normal embryonic development (53). Thus, tyrosine phosphorylation of focal contact proteins may play a role in the normal function of the cytoskeleton. Application of beads to cultured muscle cells may lead to the phosphorylation and accumulation of focal contact/postsynaptic proteins and to the development of adhesive specializations which result in the aggregation of AChRs. In a similar manner, the bead-induced PY accumulation displayed by fibroblast-like cells in this study may be due to the development of focal contacts at sites of bead contact.

Tyrosine Kinases and Their Substrates

A second class of candidates for tyrosine phosphorylation at AChR clusters are proteins involved in signal transduction by receptor or nonreceptor tyrosine kinases. Given our previous results, we have postulated that bFGF-, as well as polycation- and uncoated beads activate specific receptor tyrosine kinases, resulting in cluster formation via activation of a second messenger system or an intracellular phosphorylation cascade (6, 42). Phosphorylation of the AChR or associated proteins by receptor tyrosine kinases or downstream kinases could induce self-aggregation of the receptor, or induce its association with other proteins.

Included in this class of possible substrates for tyrosine phosphorylation is the putative agrin receptor, which has been initially characterized in terms of saturable binding of agrin to the plasma membrane (35). The agrin receptor itself may be a transmembrane tyrosine kinase, or agrin binding may regulate association of the agrin receptor with a cytoplasmic tyrosine kinase. Beads and agrin may activate similar or converging signal transduction pathways, leading to tyrosine phosphorylation of similar intracellular targets.

Interestingly, a recently identified 90-kD protein recognized by anti-*src* antibodies has been shown to colocalize with AChRs at postsynaptic sites, and a similarly distributed 90-kD protein is also recognized by an anti-PY antibody (Wagner, K. R., S. L. Swope, and R. L. Huganir. 1991. *Soc. Neurosci. Abstr.* 17:22). It remains to be determined whether this protein is a tyrosine kinase and/or a cytoskeletal target for phosphorylation, and whether it is involved in AChR clustering or other aspects of postsynaptic development.

Nerve-induced AChR Clustering

With respect to the induction of postsynaptic differentiation

by nerve, it is possible that the presentation of a nerve-derived or extracellular matrix-bound factor to specific cell-surface receptors results in the rapid activation of a tyrosine kinase signal transduction system, aspects of which may be unique to this interaction. Nerve-released or cell-surface proteoglycans might act to store or present such a signal (13, 50). Alternatively, nerve might release a matrix-bound factor by proteolysis (1, 33). The initial tyrosine kinase activation could induce early events such as AChR aggregation via phosphorylation of the receptor or associated proteins, and progress to activated second messenger systems which could play a role in developing additional specializations which are dependent upon protein synthesis.

In summary, a protein tyrosine kinase(s) of the receptor or nonreceptor type appears to be involved in the early stages of bead-induced AChR cluster formation, and tyrosine phosphorylation is a common feature at clusters induced by several different stimuli. Whether these disparate stimuli act via the same signal transduction pathway, or converge at molecular steps further downstream remains to be elucidated. Further biochemical studies to determine the identity of endogenous tyrosine kinases (and phosphatases), as well as substrates which are relevant to the clustering process will undoubtedly contribute significantly to our understanding of AChR clustering and postsynaptic differentiation.

We thank Dr. Stanley Froehner for the mAb 88b, Dr. Robert Sealock for advice on the fluorescence amplification experiments, and Dr. Robert Sealock, Dr. Stanley Froehner, and Mr. Harry Weber for helpful comments and critical reading of an earlier version of this paper.

This work was supported by National Institutes of Health grant NS 23583.

Received for publication 3 June 1992 and in revised form 22 August 1992.

References

1. Anderson, M. J. 1986. Nerve-induced remodeling of muscle basal lamina during synaptogenesis. *J. Cell Biol.* 102:863–877.
2. Anderson, M. J., and M. W. Cohen. 1977. Nerve-induced and spontaneous redistribution of acetylcholine receptors on cultured muscle cells. *J. Physiol.* 268:757–773.
3. Anderson, M. J., M. W. Cohen, and E. Zorychta. 1977. Effects of innervation on the distribution of acetylcholine receptors on cultured muscle cells. *J. Physiol.* 268:731–756.
4. Anderson, M. J., S. Champaneria, and L. Swenarchuk. 1991. Synaptic differentiation can be evoked by polymer microbeads that mimic localized pericellular proteolysis by removing proteins from adjacent surfaces. *Dev. Biol.* 147:464–479.
5. Axelrod, D. 1980. Crosslinkage and visualization of acetylcholine receptors on myotubes with biotinylated α-bungarotoxin and fluorescent avidin. *Proc. Natl. Acad. Sci. USA.* 77:4823–4827.
6. Baker, L. P., Q. Chen, and H. B. Peng. 1992. Induction of acetylcholine receptor clustering by native polystyrene beads: implication of an endogenous muscle-derived signaling system. *J. Cell Sci.* 102:543–555.
7. Bloch, R. J., and Z. W. Hall. 1983. Cytoskeletal components of the vertebrate neuromuscular junction: vinculin, α-actinin, and filamin. *J. Cell Biol.* 97:217–223.
8. Bloch, R. J., and D. W. Pumplin. 1988. Molecular events in synaptogenesis: nerve-muscle adhesion and postsynaptic differentiation. *Am. J. Physiol.* 254:C345–C364.
9. Bloch, R. J., and W. G. Resneck. 1986. Actin at receptor-rich domains of isolated acetylcholine receptor clusters. *J. Cell Biol.* 102:1447–1458.
10. Bozyczko, D., C. Decker, J. Muschler, and A. Horwitz. 1989. Integrin on developing and adult skeletal muscle. *Exp. Cell Res.* 183:72–91.
11. Bridgman, P. C., and Y. Nakajima. 1983. Distribution of filipin-sterol complexes on cultured muscle cells: cell-substratum contact areas associated with acetylcholine receptor clusters. *J. Cell Biol.* 96:363–372.
12. Burridge, K., K. Fath, T. Kelly, G. Nuckolls, and C. Turner. 1988. Focal adhesions: transmembrane junctions between the extracellular matrix and the cytoskeleton. *Annu. Rev. Cell Biol.* 4:487–525.
13. Carlson, S. S., and T. N. Wight. 1987. Nerve terminal anchorage protein 1 (TAP-1) is a chondroitin sulfate proteoglycan: biochemical and electron microscopic characterization. *J. Cell Biol.* 105:3075–3086.
14. Changeaux, J.-P., A. Devillers-Thiery, and P. Chemouilli. 1984. Acetylcholine receptor: an allosteric protein. *Science (Wash. DC).* 225:1335–1345.
15. Connolly, J. A. 1984. Role of the cytoskeleton in the formation, stabilization, and removal of acetylcholine receptor clusters in cultured muscle cells. *J. Cell Biol.* 99:148–154.
16. Couteaux, R., and M. Pecot-Dechavassine. 1968. Particularites structurales du sarcoplasme sous-neural. *C.R. Acad. Sci. (Paris).* 266:D8–D10.
17. Davis, S., M. L. Lu, S.-H. Lo, S. Lin, J. A. Butler, B. J. Druker, T. M. Roberts, Q. An, and L.-B. Chen. 1991. Presence of an SH2 domain in the actin-binding protein tensin. *Science (Wash. DC).* 252:712–715.
18. DeClue, J. E., and G. S. Martin. 1987. Phosphorylation of talin at tyrosine in Rous sarcoma virus-transformed cells. *Mol. Cell. Biol.* 7:371–378.
19. Ferns, M. J., and Z. W. Hall. 1992. How many agrins does it take to make a synapse? *Cell.* 70:1–3.
20. Fertuck, H. C., and M. M. Salpeter. 1976. Quantitation of junctional and extrajunctional acetylcholine receptors by electron microscopic autoradiography after ^{125}I-α-bungarotoxin binding at mouse neuromuscular junctions. *J. Cell Biol.* 69:144–158.
21. Froehner, S. C. 1991. The submembrane machinery for nicotinic acetylcholine receptor clustering. *J. Cell Biol.* 114:1–7.
22. Glenney, J. R., and L. Zokas. 1989. Novel tyrosine kinase substrates from Rous sarcoma virus-transformed cells are present in the membrane skeleton. *J. Cell Biol.* 108:2401–2408.
23. Hall, Z. W., B. W. Lubit, and J. H. Schwartz. 1981. Cytoplasmic actin in postsynaptic structures at the neuromuscular junction. *J. Cell Biol.* 90:789–792.
24. Hirst, R., A. Horwitz, C. Buck, and L. Rohrschneider. 1986. Phosphorylation of the fibronectin receptor complex in cells transformed by oncogenes that encode tyrosine kinases. *Proc. Natl. Acad. Sci. USA.* 83:6470–6474.
25. Huganir, R. L., and P. Greengard. 1983. cAMP-dependent protein kinase phosphorylates the nicotinic acetylcholine receptor. *Proc. Natl. Acad. Sci. USA.* 80:1130–1134.
26. Huganir, R. L., and P. Greengard. 1987. Regulation of receptor function by protein phosphorylation. *Trends Pharmacol. Sci.* 8:472–477.
27. Huganir, R. L., and P. Greengard. 1990. Regulation of neurotransmitter receptor desensitization by protein phosphorylation. *Neuron.* 5:555–567.
28. Huganir, R. L., K. Miles, and P. Greengard. 1984. Phosphorylation of the nicotinic acetylcholine receptor by an endogenous tyrosine-specific protein kinase. *Proc. Natl. Acad. Sci. USA.* 81:6968–6972.
29. Ito, S., D. K. Werth, N. D. Richert, and I. Pastan. 1983. Vinculin phosphorylation by the *src* kinase. *J. Biol. Chem.* 258:14626–14631.
30. Luther, P. W., and R. J. Bloch. 1989. Formaldehyde-amine fixatives for immunocytochemistry of cultured *Xenopus* muscle cells. *J. Histochem. Cytochem.* 37:75–82.
31. Luther, P. W., and H. B. Peng. 1985. Membrane-related specializations associated with acetylcholine receptor aggregates induced by electric fields. *J. Cell Biol.* 100:235–244.
32. Maher, P. A., E. B. Pasquale, J. Y. J. Wang, and S. J. Singer. 1985. Phosphotyrosine-containing proteins are concentrated in focal adhesions and intercellular junctions in normal cells. *Proc. Natl. Acad. Sci. USA.* 82:6576–6580.
33. McGuire, P. G., and N. W. Seeds. 1990. Degradation of underlying extracellular matrix by sensory neurons during neurite outgrowth. *Neuron.* 4:633–642.
34. Miles, K., P. Greengard, and R. L. Huganir. 1989. Calcitonin gene-related peptide regulates phosphorylation of the nicotinic acetylcholine receptor in rat myotubes. *Neuron.* 2:1517–1524.
35. Nastuk, M. A., E. Lieth, J. Ma, C. A. Cardasis, E. B. Moynihan, B. A. McKechnie, and J. R. Fallon. 1991. The putative agrin receptor binds ligand in a calcium-dependent manner and aggregates during agrin-induced acetylcholine receptor clustering. *Neuron.* 7:807–818.
36. Olek, A. J., P. A. Pudimat, and M. P. Daniels. 1983. Direct observation of the rapid aggregation of acetylcholine receptors on identified cultured myotubes after exposure to embryonic brain extract. *Cell.* 34:255–264.
37. Orida, N., and M.-M. Poo. 1978. Electrophoretic movement and localisation of acetylcholine receptors in the embryonic muscle cell membrane. *Nature (Lond.).* 275:31–35.
38. Pasquale, E. B., P. A. Maher, and S. J. Singer. 1986. Talin is phosphorylated on tyrosine in chicken embryo fibroblasts transformed by Rous sarcoma virus. *Proc. Natl. Acad. Sci. USA.* 83:5507–5511.
39. Peng, H. B. 1987. Development of the neuromuscular junction in tissue culture. *CRC Crit. Rev. Anat. Sci.* 1:91–131.
40. Peng, H. B., and P.-C. Cheng. 1982. Formation of postsynaptic specializations induced by latex beads in cultured muscle cells. *J. Neurosci.* 2:1760–1774.
41. Peng, H. B., and K. A. Phelan. 1984. Early cytoplasmic specialization at the presumptive acetylcholine receptor cluster: a meshwork of thin filaments. *J. Cell Biol.* 99:344–349.
42. Peng, H. B., L. P. Baker, and Q. Chen. 1991. Induction of synaptic development in cultured muscle cells by basic fibroblast growth factor. *Neuron.* 6:237–246.
43. Peng, H. B., L. P. Baker, and Q. Chen. 1991. Tissue culture of *Xenopus*

neurons and muscle cells as a model for studying synaptic induction. *In* Methods in Cell Biology. v. 36. *Xenopus laevis*: Practical Uses in Cell and Molecular Biology. B. K. Kay and H. B. Peng, editors. Academic Press, New York. 511–526.

43a. Peng, H. B., L. P. Baker, and Z. Dai. 1993. A role of tyrosine phosphorylation in the formation of acetylcholine receptor clusters induced by electric fields in cultured *Xenopus* muscle cells. *J. Cell Biol.* 120:197–204.

44. Prives, J., A. B. Fulton, S. Penman, M. P. Daniels, and C. N. Christian. 1982. Interaction of the cytoskeletal framework with acetylcholine receptor on the surface of embryonic muscle cells in culture. *J. Cell Biol.* 92:231–236.

45. Qu, Z., E. Moritz, and R. L. Huganir. 1990. Regulation of tyrosine phosphorylation of the nicotinic acetylcholine receptor at the rat neuromuscular junction. *Neuron.* 2:367–378.

46. Safran, A., R. Sagir-Eisenberg, D. Neumann, and S. Fuchs. 1987. Phosphorylation of the acetylcholine receptor by protein kinase C and identification of the phosphorylation site within the receptor δ subunit. *J. Biol. Chem.* 262:10506–10510.

47. Schroeder, W., H. E. Meyer, K. Buchner, H. Bayer, and F. Hucho. 1991. Phosphorylation sites of the nicotinic acetylcholine receptor: a novel site detected in position δ-S362. *Biochem.* 30:3583–3588.

48. Sealock, R., B. Paschal, M. Beckerle, and K. Burridge. 1986. Talin is a post-synaptic component of the rat neuromuscular junction. *Exp. Cell Res.* 163:143–150.

49. Sefton, B. M., T. Hunter, E. H. Ball, and S. J. Singer. 1981. Vinculin: a cytoskeletal target of the transforming protein of Rous sarcoma virus. *Cell.* 24:165–174.

50. Stadler, H., and M.-L. Kiene. 1987. Synaptic vesicles in electromotoneurones. II. heterogeneity of populations is expressed in uptake properties; exocytosis and insertion of a core proteoglycan in the extracellular matrix. *EMBO (Eur. Mol. Biol. Organ.) J.* 6:2217–2221.

51. Stollberg, J., and S. E. Fraser. 1988. Acetylcholine receptors and concanavalin A-binding sites on cultured *Xenopus* muscle cells: electrophoresis, diffusion, and aggregation. *J. Cell Biol.* 107:1397–1408.

52. Tank, D. W., E.-S. Wu, and W. W. Webb. 1982. Enhanced molecular diffusibility in muscle blebs: release of lateral constraints. *J. Cell Biol.* 92:207–212.

53. Turner, C. E. 1991. Paxillin is a major phosphotyrosine-containing protein during embryonic development. *J. Cell Biol.* 115:201–207.

54. Turner, C. E., N. Kramarcy, R. Sealock, and K. Burridge. 1991. Localization of paxillin, a focal adhesion protein, to smooth muscle dense plaques, and the myotendinous and neuromuscular junctions of skeletal muscle. *Exp. Cell Res.* 192:651–655.

55. Usdin, T. B., and G. D. Fischbach. 1986. Purification and characterization of a polypeptide from chick brain that promotes the accumulation of acetylcholine receptors in chick myotubes. *J. Cell Biol.* 103:493–507.

56. Wallace, B. G., Z. Qu, and R. L. Huganir. 1991. Agrin induces phosphorylation of the nicotinic acetylcholine receptor. *Neuron.* 6:869–878.

57. Yarden, Y., and A. Ullrich. 1988. Growth factor receptor tyrosine kinases. *Annu. Rev. Biochem.* 57:443–478.